



Comparative study on the preparation of belite cement from nano-silicas extracted from different agricultural wastes with calcium carbide residue

Kittipong Kunchariyakun, Suthatip Sinyoung, Suwimol Asavapisit & Kenneth J. D. MacKenzie

To cite this article: Kittipong Kunchariyakun, Suthatip Sinyoung, Suwimol Asavapisit & Kenneth J. D. MacKenzie (2022): Comparative study on the preparation of belite cement from nano-silicas extracted from different agricultural wastes with calcium carbide residue, Journal of Sustainable Cement-Based Materials, DOI: [10.1080/21650373.2021.2025164](https://doi.org/10.1080/21650373.2021.2025164)

To link to this article: <https://doi.org/10.1080/21650373.2021.2025164>



Published online: 23 Jan 2022.



Submit your article to this journal [↗](#)



Article views: 61




View related articles [↗](#)



View Crossmark data [↗](#)



Comparative study on the preparation of belite cement from nano-silicas extracted from different agricultural wastes with calcium carbide residue

Kittipong Kunchariyakun^{a,b} , Suthatip Sinyoung^{c*}, Suwimol Asavapisit^d and Kenneth J. D. MacKenzie^e

^aSchool of Engineering and Technology, Walailak University, Thai Buri, Thailand; ^bCenter of Excellence in Sustainable Disaster Management, Walailak University, Thai Buri, Thailand; ^cDepartment of Civil and Environmental Engineering, Faculty of Engineering, Prince of Songkla University, Hat Yai, Thailand; ^dSchool of Energy, Environment and Materials, King Mongkut's University of Technology Thonburi, Bangkok, Thailand; ^eSchool of Chemical and Physical Science, Victoria University of Wellington, MacDiarmid Institute for Advanced Materials and Nanotechnology, Wellington, New Zealand

Belite cement was prepared using nano-silicas extracted from three different agricultural wastes – black rice husk ash (BRHA), bagasse ash (BA), and palm oil fuel ash (POFA) – which were reacted at 1200 – 1400 °C with CaC₂ residue as calcium source. The product was compared with that from CaCO₃. Nano-silica extracted from BRHA was of very fine particle size (surface area 312.4 m²/g and V/S ratio 0.35 × 10⁶ cm) and being highly reactive, forms β-C₂S at lower firing temperatures; however, at higher temperatures, less-desirable γ-polymorphs are formed. Nano-silica extracted from POFA contains Na₂O, Al₂O₃, and K₂O impurities, which stabilize the β and α-forms and delay the transformation to γ-phase. This is reflected in relatively high compressive strength at firing temperature above 1200 °C, compared to other mixtures. Thus, these results indicate that the best combination of these waste materials for the preparation of belite cement phases is POFA ash and CaC₂ residue.

Keywords: Belite cement; nano-silica; ashes; calcium carbide residue; agricultural wastes

1. Introduction

Calcium silicate cement based on belite-rich clinker is an attractive and eco-friendly option. The production of belite (dicalcium silicate, C₂S, which occurs in five polymorphic forms [1]) requires a relatively low energy input (~1350 kJ/kg⁻¹) [2] and produces low CO₂ emissions [3] compared to tricalcium silicate, one of the other components of Portland cement. However, a major drawback to belite cement is its slow rate of hydration and low early-stage strength development. Of the five polymorphic forms of C₂S (Figure 1), the β and γ-forms are formed at a low temperature but only the β-form is hydraulically active [4]. Several studies of belite cement formation have aimed to improve its properties; these include the use of gel and spray drying [5], the use of very reactive forms of calcium and silica starting materials [6,7], and hydrothermal pretreatment [8–10].


Recently, nanotechnology has attracted increasing attention as a means of enhancing the compressive strength, durability, and workability of cement and concrete; this arises from the particle size effects on the nano-structure, surface, quantum effects (confinement of the movement of electrons), and interface effects (the interaction between nano-materials and other components) [11–13]. Since silica is a major component of cement and concrete, the effect of nano-silica on the properties of cement and concrete is of considerable interest. Previous research has shown that the use of nano-silica in cement and concrete phases can improve the mechanical and

microstructural properties and produce greater pozzolanic activity than silica fume [14–17]. The performance of silica fume can be improved by various treatments to reduce the degree of densification/agglomeration [18–20]. This high reactivity and fine particle size suggests that nano-silica should be an excellent raw material for belite (dicalcium silicate) cement production.

We have successfully prepared belite cement at temperatures as low as 800 °C by the reaction of calcium nitrate with nano-silica extracted from both synthetic and real rice husk ashes; but when using a more traditional calcium source (calcium carbonate, CaCO₃), only a small proportion of β-C₂S (>50%) was formed, even at 1100 °C [7].

Silica is well known as a major component of agricultural wastes such as rice husk ash, bagasse ash, and palm oil fuel ash. These wastes are mostly disposed of in landfills, with the potential to cause major issues for environmental sustainability in term of soil contamination, leachate production, and air pollution. For this reason, these wastes have been used in various applications such as ceramic products [21], clay bricks [22,23], and additives in cement and concrete [24–29]. Nano-silica has even greater potential in other applications such as pharmaceuticals, catalysts, and chromatography [30–32], and its extraction from agricultural wastes has been researched for many years. Extraction of nano-silica from these wastes can be achieved by various methods, of which the precipitation method is more commonly favored because

*Corresponding author. Email: ssuthatip@eng.psu.ac.th

 Supplemental data for this article is available online at <https://doi.org/10.1080/21650373.2021.2025164>.

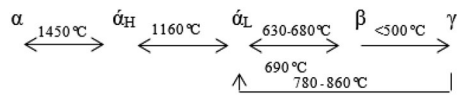


Figure 1. The five polymorphs of C_2S existing at ordinary pressure.

it is a simple process with low energy requirements [33]. This method involves chemical extraction of the silica to precipitate an aquagel which is dried to produce the nano-silica [33]. However, it has been reported [10] that the yields of nano-silica extracted by the precipitation method depend on the type of agricultural waste, each one of which can contain different components such as CaO , K_2O , Al_2O_3 , and Fe_2O_3 [34].

The calcium source used in these experiments is also a waste byproduct, calcium carbide (CaC_2) residue (CCR); this is a byproduct obtained from the production of acetylene gas (C_2H_2), which is widely used for the ripening of fruit and in the welding industry. The byproduct (calcium carbide residue) is often discarded as a highly alkaline ($pH > 12$) waste in landfills to the detriment of the environment. Recently, the demand for calcium carbide for acetylene gas production in Thailand has risen to 18,000 tons/year, producing 21,500 tons/year of calcium carbide residue; this amount is increasing every year [35]. Some researchers have used calcium carbide residue to replace cement in construction applications, and it is also mixed with waste ash [36,37] to produce a cementitious material. Wang et al. [38] studied the use of calcium carbide slag as a calcium source for cement clinker production, and reported that this is a potentially useful application. However, researchers are still searching for new ways to recycle CCR [39,40] to minimize the quantities going to landfills and thus reduce the environmental impact. The aim of the present research is to recycle CCR waste by investigating its use as a calcium oxide source to replace limestone ($CaCO_3$) in the production of belite (calcium silicate) cement, in combination with three different nano-silicas extracted from agricultural wastes as the silica sources, i.e. black rice husk ash (BRHA), bagasse ash (BA), and palm oil fuel ash (POFA). Here, we report on the mechanisms of belite cement formations from these various mixtures by using X-ray diffraction (XRD) in terms of both qualitative and quantitative analysis and by compressive strength measurements.

2. Experimental methodology

2.1. Preparation and characterization of the nano-silicas

Black rice husk ash (BRHA), bagasse ash (BA), and palm oil fuel ash (POFA) were obtained from the Thanakit Rice Mill, the Banpong Sugar Co., Ltd., and the Chumporn Palm Oil Industry, Thailand, respectively. The extraction of nano-silica from these ashes was by carried out according to Sinyoung et.al. (2017) [7] by pretreatment with hot HCl, washed with distilled water, followed by soaking in 1.5 M NaOH solution with a solid/liquid ratio of 1:6 with

constant stirring, then heating at $100^\circ C$ for 1 h. The resulting solutions were centrifuged to remove any solid residue and filtered several times to obtain clear and colorless solutions which were adjusted to $pH 7.0 \pm 0.1$ by the addition of 1.0 M HCl, and then cured at $50^\circ C$ for 12 h. The cured aquagels were centrifuged with distilled water to remove any salts, dried at $80^\circ C$ for 48 h, and then, ground and screened through a #200 mesh sieve to obtain the nano-silica powders. The particle sizes of these silicas were investigated in the nanometer range by transmission electron microscopy (TEM) using a JEM2100 microscope at an accelerating voltage of 80 kV. The samples were prepared by ultrasonically dispersing 0.2 g in ethanol, placing a drop of the suspension on a copper grid, and coating with a carbon film. The surface areas and porosities of the raw ashes and corresponding nano-silicas were measured by the BET method using a Quantachrome autosorb automated gas sorption analyzer, on 5 replicates of the N_2 adsorption isotherms.

The chemical compositions of both the raw materials and extracted nano-silica powders, determined by X-ray fluorescence (Philips model WDXRF PW2400 spectrometer), are shown in Table 1, which also includes their porosity data. The crystalline phases of all the samples were determined by X-ray diffraction using a Miniflex diffractometer with Cu $K\alpha$ radiation ($\lambda = 1.5406 \text{ \AA}$) at a voltage of 40 kV and 40 mA and a step size of $0.02^\circ 2\theta$, scanning rate of $3^\circ/\text{min}$, from 10° to $90^\circ 2\theta$.

2.2. Synthesis of the belite cement

Belite cements were synthesized with a Ca/Si ratio of 2:1 [7] by reacting each of the above three nano-silicas with CCR (calcium carbide residue, CaC_2) obtained from an acetylene gas production factory in Samutsakorn Province, Thailand. The CCR is shown by XRD (Figure 2) to contain crystalline calcium aluminium oxide carbonate sulfide hydrate ($Ca_4Al_2O_6(CO_3)_{0.67}(SO_3)_{0.33} \cdot 11H_2O$, JCPDS file no 41-0476), quartz (SiO_2 , JCPDS file no 65-0466), calcium carbonate ($CaCO_3$, JCPDS file no 05-0586), and portlandite ($Ca(OH)_2$, JCPDS file no 72-0156). The CCR was dried at $100^\circ C$ for 24 h and ground in a Los Angeles abrasion machine before being sieved to pass a 40 mesh. For comparison, an analogous set of samples was prepared using the more conventional Ca source, laboratory grade $CaCO_3$ (CC) (Ajax Finechem). Each mixture as described in Table 2 was mechanically mixed for 5 min, and then, pretreated by autoclaving at $200 \pm 3^\circ C$ for 5 h before firing in an electric furnace at $1200^\circ C$, $1300^\circ C$, and $1400^\circ C$ for 1 h. After firing, the samples were rapidly cooled by quenching the crucible in cold water, then ground to pass a 200-mesh sieve, and analyzed to determine their crystalline components by XRD. The X-ray data were also used to quantitatively determine the crystalline phases using the computer program TOPAS 2.1. The goodness-of-fit is indicated by the weight-profile R_{wp} , which is deemed to be satisfactory at values < 15 . Free lime in the samples was determined according to the test method ASTM C 114-07 [41].

Table 1. Chemical composition and pore characteristics of the raw and extracted silicas.

Details	BRHA		BA		POFA	
	Raw	Extracted	Raw	Extracted	Raw	Extracted
SiO ₂	93.70	94.46	68.60	94.23	29.13	89.44
Na ₂ O	0.03	4.43	1.07	3.01	0.38	2.24
K ₂ O	2.55	0.90	3.92	0.43	25.41	4.21
Al ₂ O ₃	0.40	0.15	3.97	2.11	1.00	3.86
CaO	0.92	0.04	7.85	0.10	11.90	0.02
Fe ₂ O ₃	0.28	0.02	3.16	0.10	1.38	0.03
Cl	–	–	0.95	–	7.57	–
P ₂ O ₅	–	–	1.71	–	5.76	–
MgO	–	–	1.69	–	4.02	–
TiO ₂	0.02	–	0.27	–	0.07	–
MnO	–	–	0.14	–	0.77	–
SO ₃	0.04	–	1.44	–	9.52	–
LOI ^a	4.40	–	5.22	–	3.10	–
Surface area (S, m ² /g)	5.157	312.4	14.79	403.9	5.095	323
Total Pore volume (V, cm ³ /g)	0.01652	1.094	0.0335	0.5927	0.0087	0.7808
V/S (10 ⁻⁶ cm)	0.320	0.350	0.227	0.147	0.171	0.242

^aLoss on ignition.

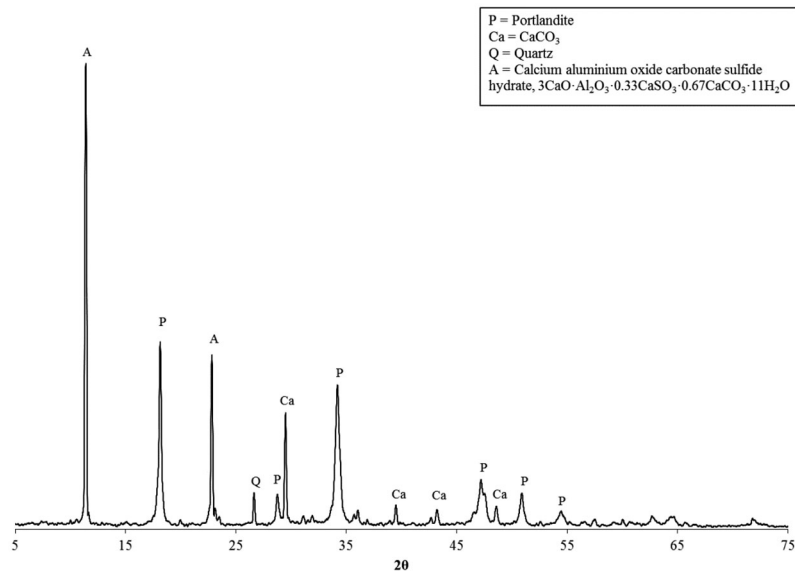
Figure 2. XRD pattern of CaC₂ residue.

Table 2. Details of the sample mixtures in a 100 g/batch.

Sample code	Details	CCR (g)	CC (g)	BRHA (g)	BA (g)	POFA (g)
CRRHA	CCR + BRHA	72.35	–	27.65	–	–
CRBA	CCR + BA	72.30	–	–	27.70	–
CRPA	CCR + POFA	71.24	–	–	–	28.76
CCRHA	CC + BRHA	–	75.91	24.09	–	–
CCBA	CC + BA	–	75.87	–	24.13	–
CCPA	CC + POFA	–	74.90	–	–	25.10

2.3. Preparation of the belite cement mortar

The belite cement mortar was prepared according to ASTM C109 [42], using a cement-to-sand ratio at 1:2.75 and a water-to-cement ratio of 0.485. The sand used in this work was Ottawa 20-30 sand (U.S. Silica Company, Ottawa, Ill), with a specific gravity, median grain size, (D₅₀), uniformity coefficient, and density of 2.65,

0.71 mm, 1.20, and 17.80 (kN/m³), respectively. The belite cement and sand were weighed and mixed in a Hobart mixer for 1 min, and then added with water and mixed again for 1 min and 30 s. The slurry was poured into 5 cm cube steel molds and sealed with plastic wrap. The samples were removed from the molds after 2 days and kept at a relative humidity of more than 90%, and

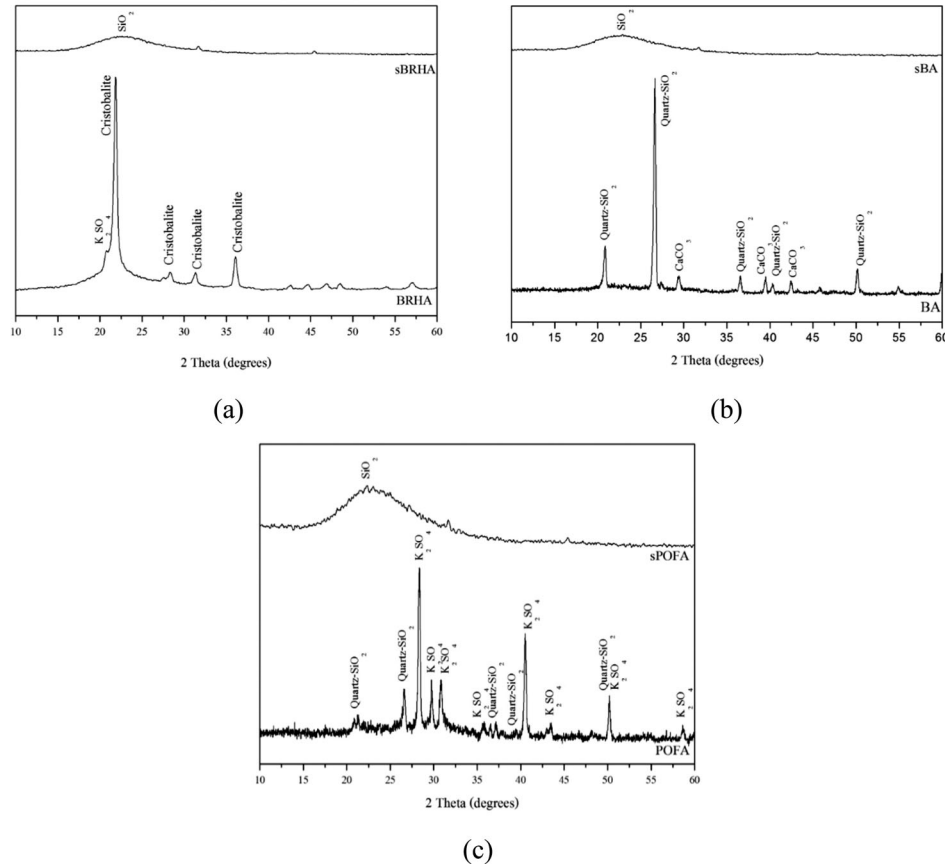


Figure 3. XRD patterns of raw and extracted nano-silicas. (a) BRHA, (b) BA, and (c) POFA.

then they were tested for compressive strength at 1, 7, 14, and 28 days.

3. Results

3.1. Mineralogical and physical properties of the raw ashes and extracted nano-silicas

The mineralogical properties of the three raw ashes and the corresponding extracted nano-silicas are shown in Figure 3. Raw BRHA contains a cristobalite reflection as the main peak (Figure 3a), whereas quartz is more pronounced in raw BA and POFA (Figure 3b,c). Other crystalline phases are K_2SO_4 in raw BRHA and POFA, and $CaCO_3$ in raw BA; these are probably associated with the potassium-rich feldspar fertilizers used in the production of these materials or as agricultural artifacts picked up by the sample during collection from the field, introduced during sample collection. The difference in the silica polymorphs arises from differences in the processing temperatures and in the heating and cooling rates [43]. After extraction, the crystalline silicas are replaced by amorphous silica (at $2\theta \approx 23^\circ$) in all the samples. The purity of the nano-silica extracted from the different sources was approximately 89–94% (Table 1).

The nanometer size range of the silica crystallites extracted from siliceous materials was determined by TEM to be 15–40 nm. The surface areas of the three nano-silicas were in the range of 312–404 m²/g, and the total pore volumes were 0.5927–1.094 cm³/g (Table 1). The differences in surface area and total pore volumes of the

nano-silicas arise from the impurities present (K_2O , Al_2O_3 , and Na_2O), which adhere to the gel matrix [7,44]. These results indicate that the total pore volume/surface area (V/S) ratios of the nano-silicas were 0.350, 0.147, and 0.242 ($\times 10^{-6}$ cm) for BRHA, BA, and POFA, respectively. Sinyoung et al. (2017) [7] have shown that the relationship between the pore volume and surface area of the nano-silica can be an indicator of its reactivity, high V/S ratios corresponding to relatively high reactivity compared with low V/S ratios. Liou and Yang (2011) [30] have suggested that pore volume reduction in the nano-silicas extracted from BRHA and POFA may result from pore blocking by impurities which adhere to the interior of the gel matrix after gelation.

3.2. Phase evolution in the heated mixtures

The formation of the crystalline phases in the heated samples was studied by XRD (Figures 4–6). In all the mixtures, relatively intense reflections were observed of lamite, β - C_2S (JCPDS file No. 33-0302), at the lowest firing temperature (1200 °C) (Figure 4). Other reflections in these samples included $CaCO_3$ (JCPDS file No. 05-0586), CaO (JCPDS file No. 37-1497), cristobalite (JCPDS file No. 39-1425), pseudowollastonite (JCPDS file No 31-0300), orthorhombic Ca_2SiO_4 (JCPDS file No. 49-1672), and hexagonal Ca_2SiO_4 (JCPDS file No. 23-1045). The crystallographic cell parameters of the orthorhombic Ca_2SiO_4 were $a = 0.50821$, $b = 1.12237$, and $c = 0.67638$, with the space group of Pbnm, indicating that this was the

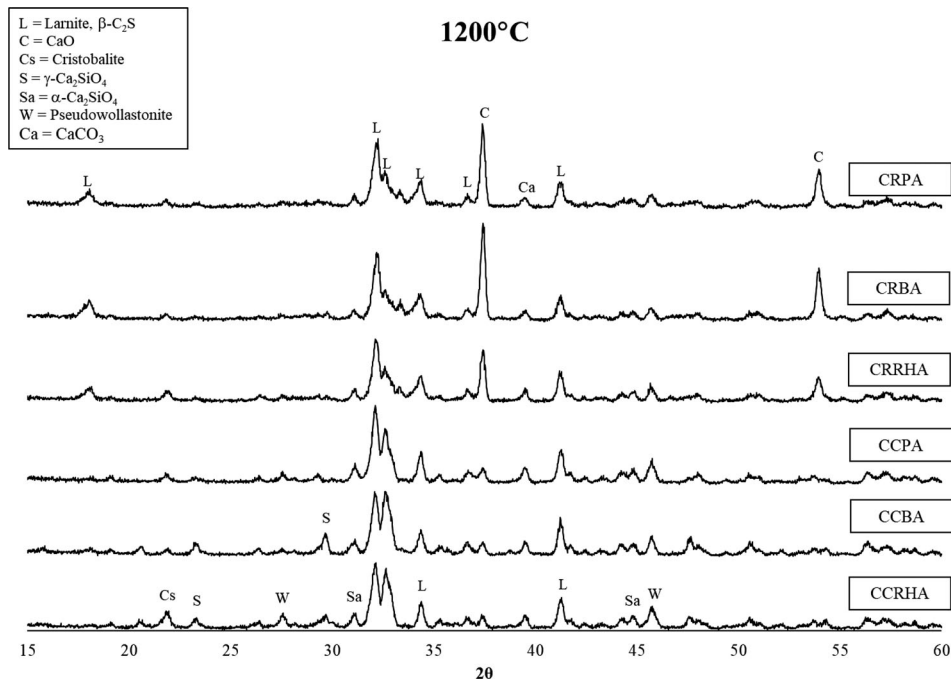


Figure 4. XRD patterns of belite cement at 1200 °C.

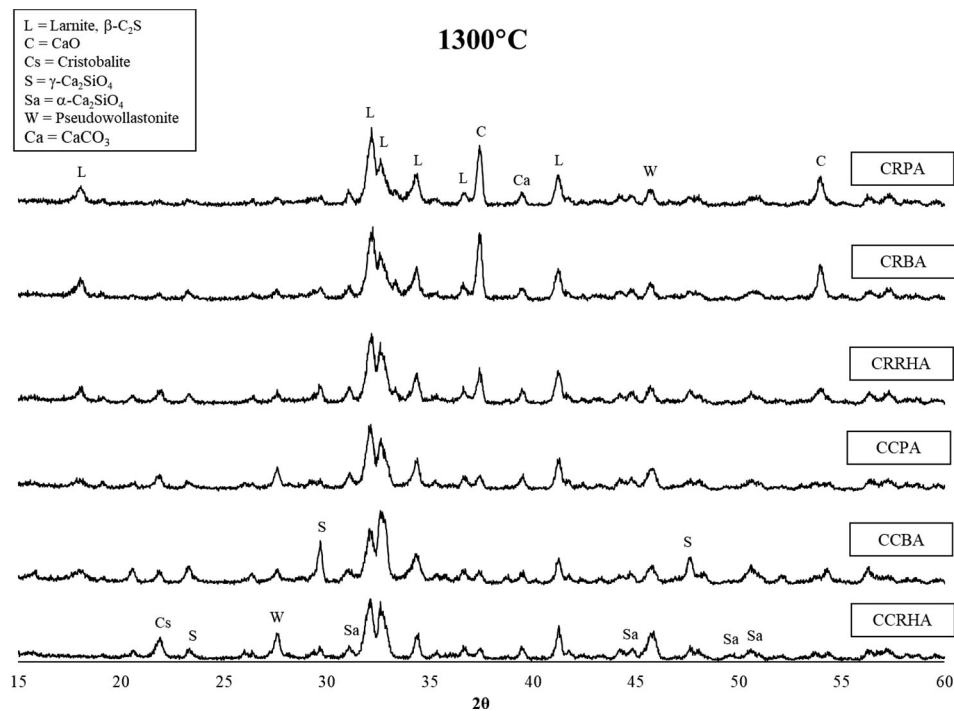


Figure 5. XRD patterns of belite cement at 1300 °C.

γ -polymorph, whereas the hexagonal polymorph was the α form [1]. Theoretically, the α -form is dominant at temperatures $>1400^\circ\text{C}$ (Figure 1). The present result indicates that high nano-silica surface areas and V/S ratios led to higher reactivity of the system, increasing the rate of reaction and forming the α -phase at relatively lower temperatures.

At the higher firing temperatures of 1300°C and 1400°C , the XRD patterns (Figures 5 and 6) showed similar behaviors, apart from a decrease in the intensity of CaO and CaCO_3 . It should be noted that there was

competition between the formation of β and γ - C_2S at $2\theta \approx 32^\circ$ and 32.5° from 1200°C to 1400°C . The peaks of γ - C_2S were of relatively low intensity at 1200°C , but as the firing temperature was increased to 1400°C , the γ -phase began to predominate over the β -phase. In cement chemistry, the transformation from β to γ - C_2S depends on many factors including the cooling rate and the calcium and silica content [1,45]. One of the most important factors relates to the fineness of the β crystallites; previous researchers have reported that β crystallites smaller than $5\mu\text{m}$ stabilize this phase when fired at temperatures

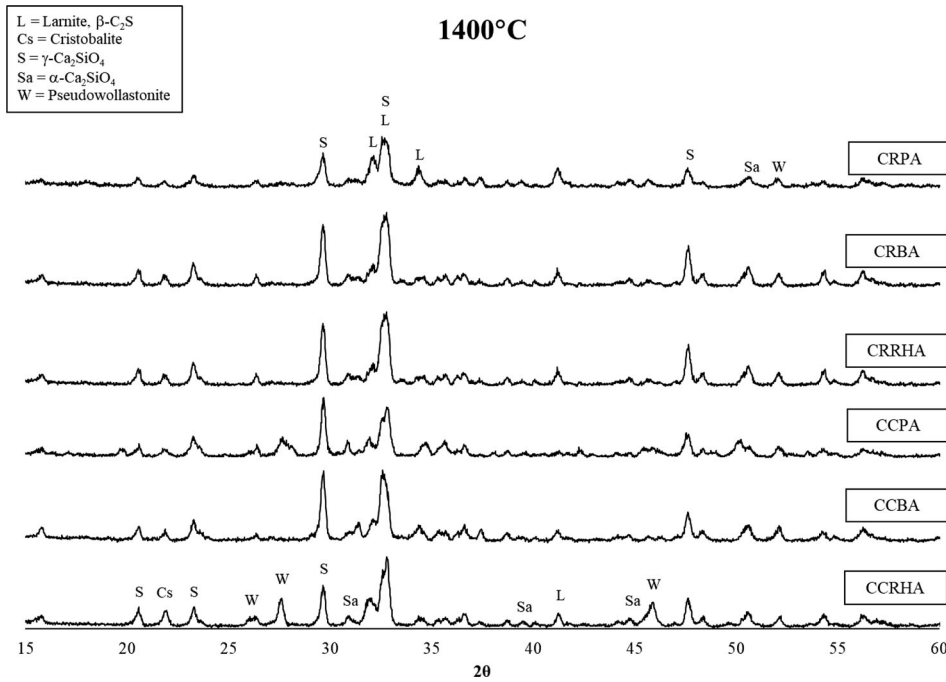


Figure 6. XRD patterns of belite cement at 1400 °C.

<1150 °C, even without stabilizers [46,47]. However, at higher firing temperatures and slow cooling, a mixture of β and γ is obtained [45]. In the case of nano-materials, it has been reported that nano-particles favor the formation of small-sized crystallites [48]. Thus, the use of nano-silica should promote the formation of small β -C₂S crystallites which should, therefore, be stable even at 1200 °C. Above 1200 °C, α -C₂S crystals may grow, resulting in the transformation of the β to γ -form during fast cooling [45].

During recrystallization of the β -phase to other phases, pseudowollastonite was also formed, especially in mixtures containing CaCO₃ as the Ca source. This indicates that β -C₂S not only transformed to the γ -phase, but also might be decomposed to pseudowollastonite at temperatures >1200 °C. El-Didamony et al. (2012) [6] also noted that wollastonite (CaSiO₃) is formed by the reaction of 2 moles of β -C₂S to form some C₃S and wollastonite at 1250 °C. In nature, the ideal composition of wollastonite is 48.3% CaO and 51.7% SiO₂, and it forms as three polymorphs (β -CaSiO₃, wollastonite-2M, and α -wollastonite or pseudowollastonite). Of these wollastonite polymorphs, the α -phase (pseudowollastonite) is stable above 1125 ± 10 °C [49,50]. As the firing temperature of this study was increased to >1200 °C, some β -C₂S and the small residual CaO content decomposed to form pseudowollastonite, which forms where the ratios of Ca:Si are < 2. Both pseudowollastonite and wollastonite have no significance for the hydraulic activity [1].

3.3. Influence of the different silica sources on the formation of belite cement

To study the effect of the three different silica sources on belite formation, the XRD patterns of the various mixtures fired at the various temperatures were used to calculate the weight fractions of the phases using the TOPAS 2.1

program. The results (Figure 7) show that the weight fraction of β -C₂S in all the mixtures was about 46–62% at the lowest firing temperature (1200 °C) and decreased with increasing temperature (Figure 7a). This decrease in β -C₂S was due to the formation of the γ and α forms, as shown in Figure 7b,c. At the same time, the content of pseudowollastonite increased with increasing temperature, except in the mixtures containing CCR fired at 1300 °C (Figure 7d). The remaining CaO and CaCO₃ contents decreased with increasing firing temperature, reflecting the formation of clinker products (Figure 7e,f).

Figure 7a shows that the β -C₂S weight fraction in the mixtures of the nano-silica extracted from BRHA reacted with both CaC₂ and CaCO₃ (samples CRRHA and CCRHA), was highest at 1200 °C, followed by POFA (samples CRPA and CCPA) and BA (samples CRBA and CCBA). However, in the mixtures prepared from the nano-silica extracted from POFA (samples CRPA and CCPA), β -C₂S formation became dominant at temperatures >1200 °C. The V/S ratios suggest that the nano-silica extracted from BRHA should be the most reactive and form β -C₂S at the lowest firing temperatures, followed by POFA and BA. β -C₂S is well known to be unstable, as reflected by the decrease in its weight fraction at increasing firing temperatures. The β -phase can be stabilized in various ways by ensuring that it is prepared to have a small crystal size, by rapidly cooling it, or by the addition of stabilizers such as Cr₂O₃, B₂O₃, Na₂O, or K₂O [45,51]. Previous researchers have reported that 0.3% of Na₂O or K₂O was sufficient to stabilize β -C₂S [52]. The chemical composition of the nano-silica extracted from POFA (Table 1) shows this to be less pure than the other silicas, containing 2.24% Na₂O, 4.21% K₂O, and 3.86% Al₂O₃. In belites formed from an impure nano-silica such as this, the Ca²⁺ can be substituted by K⁺ or Na⁺, and the SiO₄⁴⁻ by AlO₄⁵⁻, thereby stabilizing the C₂S phases [45]. The

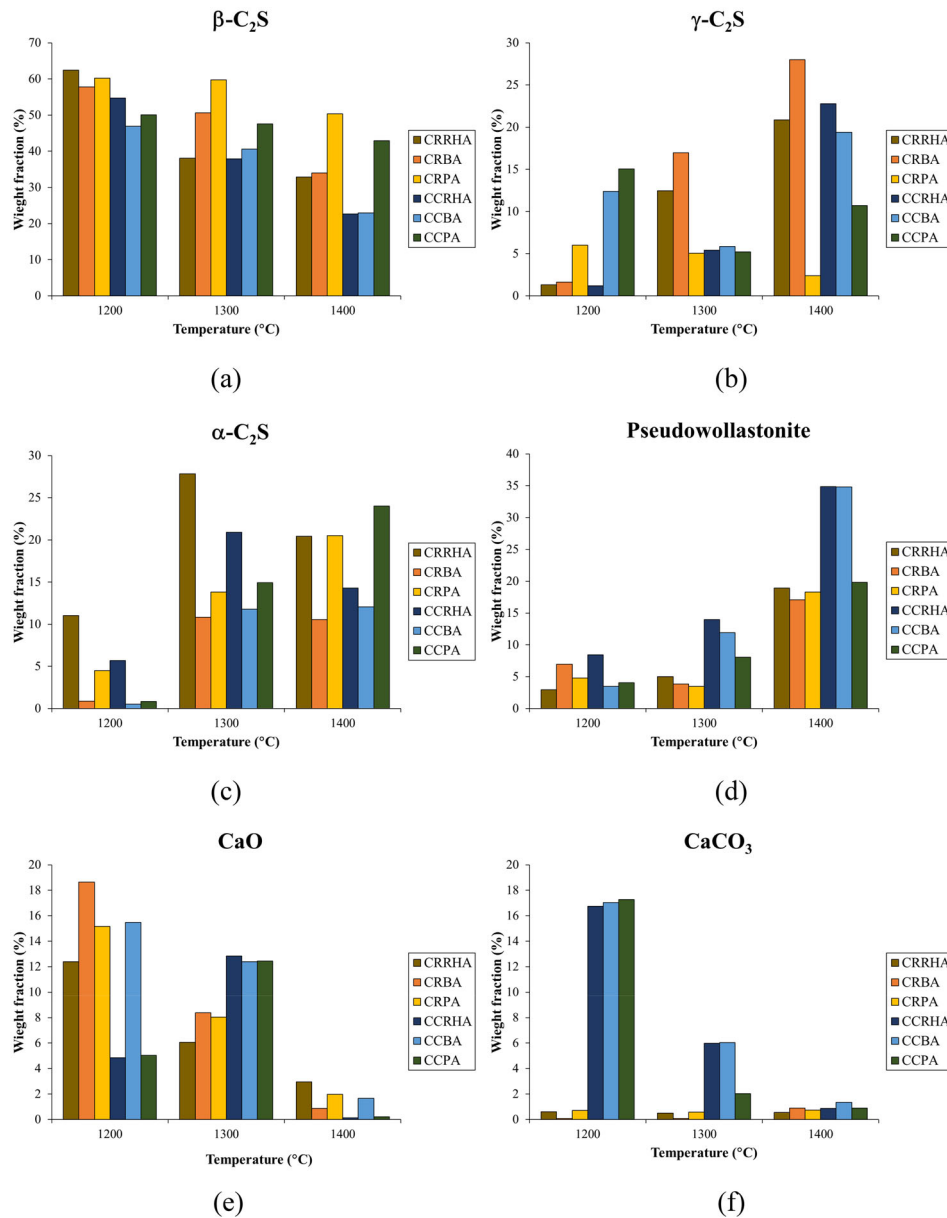


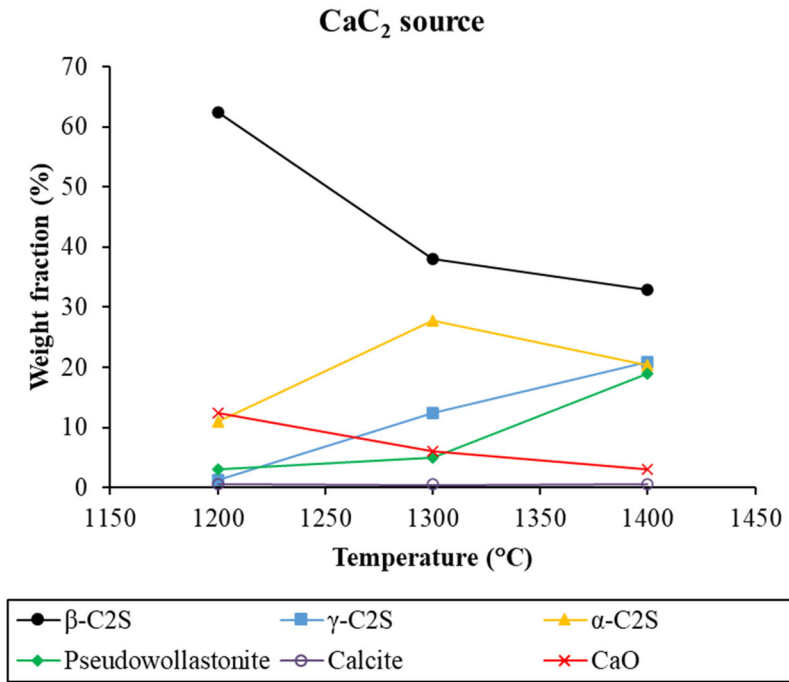
Figure 7. Weight fraction of phases in various mixtures. (a) β -C₂S, (b) γ -C₂S, (c) α -C₂S (d) pseudowollastonite, (e) CaO, and (f) CaCO₃.

presence of these impurities could explain the retardation in POFA of the β -phase transformation to other phases with increasing firing temperature.

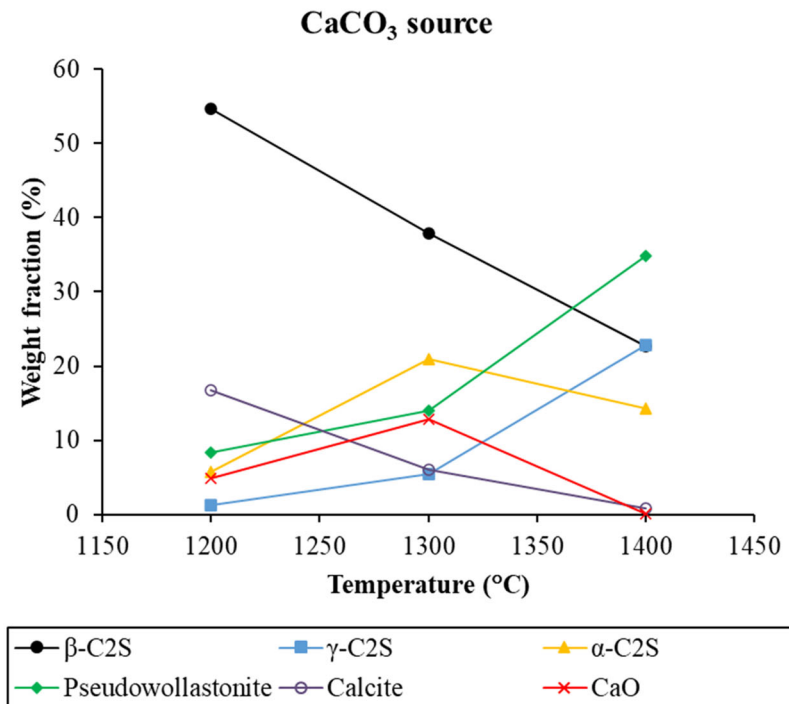
The weight fraction of α -C₂S (Figure 7c) shows the formation of increasingly high amounts of this phase in samples containing the nano-silica extracted from BRHA with increasing firing temperature up to 1300 °C. At higher firing temperatures, the most α -C₂S forms in the samples containing the nano-silica extracted from POFA. By contrast, the weight fraction of γ -C₂S in the POFA samples was highest at lower temperatures, but subsequently decreased with increasing firing temperature (Figure 7b). The greatest amount of γ -C₂S was formed in the mixture of CaC₂ and the nano-silica extracted from BA (sample CRBA). This suggests that the relatively reactive nano-silica extracted from BRHA facilitates the transformation of β to α -C₂S at low temperature and prevents the β -form from recrystallizing to γ -C₂S. However, at firing temperatures up to 1400 °C

the α -form transformed to the γ -form during cooling due to the absence of a stabilizer; by contrast, the impurities in the nano-silica extracted from POFA acted as stabilizers, preventing this recrystallization of the α -form to the γ -form. The nano-silica extracted from BA was of relatively low reactivity and contained insufficient stabilizer to hinder the transformation of β -to- α -C₂S at low firing temperatures, and subsequently recrystallized to the γ -form during cooling, especially in samples fired at 1400 °C.

The weight fraction of the pseudowollastonite (Figure 7d) shows that this phase predominated at all firing temperatures in the mixtures of the nano-silica extracted from BRHA with both CCR and CC (samples CRRHA and CCRHA), followed by the nano-silicas from BA and POFA, respectively. The mixture of POFA with calcite (sample CCPA) fired at 1400 °C contained a relatively low weight fraction of pseudowollastonite due to the stabilization of the belite phase; this suggests that



(a)



(b)

Figure 8. Phases evolution of belite cement from nano-silica extracted from BRHA. (a) with CaC₂ and (b) with CaCO₃.

pseudowollastonite formation depended on the reactivity and compositions of the raw materials, as well as the firing temperature and the Ca/Si ratio.

In the mixtures containing CaCO₃ as the calcium source, the weight fraction of CaCO₃ remained high even at 1300 °C (Figure 7f), especially in the samples containing BRHA and BA (sample CCRHA and CCBA). We

suggest that this was because the surface of the CaCO₃ was coated with very fine silica particles, which acted as barriers to CO₂ diffusion and increased the activation energy [53], retarding the decomposition of the carbonate. However, the two nano-silicas extracted from BRHA and POFA were both highly reactive and could rapidly react with the CaO formed at 1200 °C (Figure 7e).

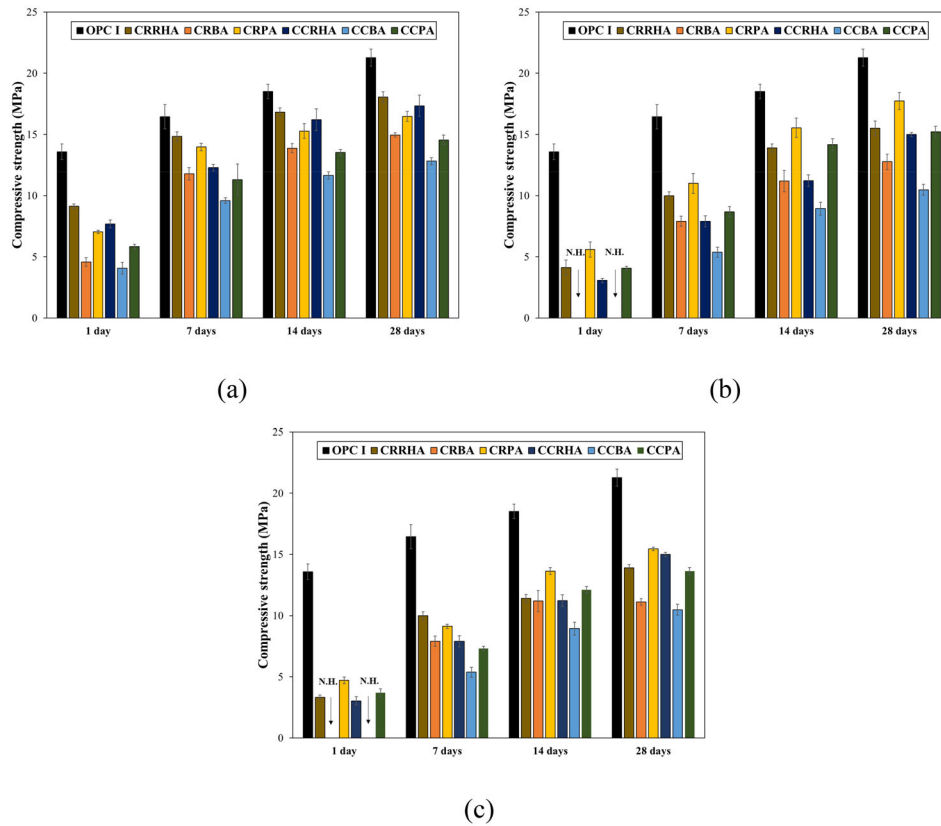


Figure 9. Compressive strength of belite cement from various mixtures. (a) at 1200 °C, (b) at 1300 °C, and (c) 1400 °C. (Note: N.H. = Non-hardened).

3.4. Influence of the calcium source on the formation mechanism of belite cement

The effect of the two different calcium sources on the formation of belite cement by reaction with the nano-silica extracted from BRHA was studied to compare the performance of an industrial waste material (calcium carbide residue) with a purer calcium source, CaCO_3 . Nano-silica from BRHA was selected for these experiments since it was shown in the previous section to form belite formation at the lowest temperatures. The results of these comparative experiments (mixtures CRRHA, containing CaC_2 and CCRHA, containing CaCO_3) indicate that both calcium sources showed very similar trends in the formation of the β , γ , and α -belite phases as a function of firing temperature (Figure 8a,b). However, the weight fraction of the pseudowollastonite formed with the CaCO_3 mixture was greater than in the mixture containing CaC_2 . The free CaO content of the CaCO_3 mixture increased up to 1300 °C and then decreased at 1400 °C (Figure 8b), but it decreased with firing temperature in the mixture containing CaC_2 (Figure 8a); this was due to the fact that the calcium in the CaC_2 is predominantly $\text{Ca}(\text{OH})_2$, which is more readily decomposed and reactive than CaCO_3 .

Theoretically, C_2S and pseudowollastonite are formed from CaO and SiO_2 in ratios of 2:1 and 1:1, respectively [45,50]. The mixture containing CaCO_3 only slowly decomposed to free CaO, even at temperatures >1300 °C. Consequently, the concentration of CaO was insufficient to form C_2S phases and was more likely to form pseudowollastonite at higher temperatures. By contrast, the CaC_2

reacted more readily to form the C_2S phases at lower firing temperatures.

Furthermore, a sulfate impurity, $3\text{CaO}\cdot\text{Al}_2\text{O}_3\cdot 0.33\text{CaSO}_3\cdot 0.67\text{CaCO}_3\cdot 11\text{H}_2\text{O}$, which was present in the CaC_2 residue, may be thermally decomposed to $[\text{SO}_4]^{2-}$; this species, along with other anions such as $[\text{AlO}_4]^{5-}$ are known to stabilize the C_2S phases by substitution of the silicate anions [45]. Thus, this impurity in the mixtures containing the CaC_2 residue should stabilize the C_2S phases and prevent their decomposition and recrystallization to the high temperature phase pseudowollastonite.

3.5. Compressive strength of the belite cement mortars

Figure 9 shows the 1-, 7-, 14-, and 28-day compressive strengths of the belite cement mortars from the various mixtures and preparation temperatures. The belite cement was also compared with the commercial ordinary Portland cement (OPC), showing that the compressive strengths of all the belite samples were relatively lower than those of OPC. At a preparation temperature of 1200 °C, the highest compressive strength was gained from the CRRHA mixture, followed by CCRHA > CRPA > CCPA > CRBA > CCBA, (Figure 9a). However, the CRPA became stronger than CRRHA at preparation temperatures of 1300 °C and 1400 °C (Figure 9b,c). The compressive strengths at 1300 °C and 1400 °C were in the order CRPA > CRRHA > CCPA > CCRHA > CRBA > CCBA. This result correlates with the weight fractions of the β , γ , and α -polymorphs of C_2S , as shown in Figure 7a,b.

Theoretically for belite cement, the β and α -C₂S polymorphs are hydraulic phases, whereas the γ -polymorph is a non-hydraulic phase [3,54], which indirectly affects the development of compressive strength. Belite cement contains a relatively higher proportion of β and α -polymorphs than γ , which can contribute to the enhancement of compressive strength. In the present research, the relatively high compressive strength of the mixtures containing the nano-silica extracted from BRHA and fired at 1200 °C resulted from a high weight fraction of β -C₂S and a low weight fraction of γ -C₂S. Although the other mixtures (except CCBA) contained $a > 50\%$ weight fraction of β -C₂S, they also contained a relatively high weight fraction of γ -C₂S compared to the CRRHA and CCRHA mixtures. This resulted in a negative effect on compressive strength. For temperatures > 1200 °C, the β -polymorph in the mixtures containing the nano-silicas extracted from BRHA and BA was transformed to another phase, especially the γ -polymorph, although the mixture containing the nano-silica extracted from POFA still had a high weight fraction of the β -polymorph. Consequently, the CRPA mixture showed the highest compressive strength. In addition, the high weight fraction of γ -C₂S and low weight fractions of β and α -C₂S in the mixtures of CRBA and CCBA at > 1200 °C produced unhardened specimens after curing for 1 day.

4. Conclusion

This work studied the formation mechanism of eco-friendly belite cement phases from three different nano-silicas derived from agricultural waste products and a calcium source from another industrial waste (CaC₂ residue). The following conclusions were drawn:

- The surface areas and impurity contents of the starting ashes affect the surface areas, pore volumes, and purity of the corresponding nano-silicas, and hence their reactivity in the formation of calcium silicate (belite) cement phases.
- The preferred form of C₂S for belite cement is the β -form which is hydraulically active. At higher firing temperatures, β -C₂S transforms to the less desirable γ -form, but the impurities in the nano-silica extracted from palm oil fuel ash (POFA) stabilize the β and α -polymorphs and delay the transformation to the γ -phase.
- The nano-silica extracted from rice husk ash (BRHA) is of very fine particle size, and is thus highly reactive, forming β -C₂S at low temperatures; however, at higher firing temperatures, this phase reverts to the less desirable polymorphs.
- Both CaC₂ residue and CaCO₃ show very similar trends in the formation of β , γ , and α -C₂S as a function of the firing temperature. However, the weight fraction of the less desirable pseudowollastonite formed by the reaction of less-reactive CaCO₃ with reactive BRHA nano-silica is greater than with the CaC₂ residue. This is possibly due

to the fact that the very fine nano-silica covers the CaCO₃ particles, slowing their decomposition and directly affecting the formation of the pseudowollastonite.

- The stabilization of β -C₂S in the mixture containing the nano-silica extracted from POFA produces a material with a relatively high compressive strength, especially when combined with the CaC₂ residue.
- These results indicate that the best of these waste materials for the preparation of belite cement is the reaction of palm oil fuel ash with CaC₂ residue.

Acknowledgements

The authors acknowledge the financial support provided by engineering faculty research fund, Prince of Songkla university (Grant No.: ENG6204107S), Thailand Science Research and Innovation Contact No. IRN62W0005 and the new strategic research project (P2P), Walailak University, Thailand.

Disclosure statement

No potential conflict of interest was reported by the authors.

Funding

The authors acknowledge the financial support provided by engineering faculty research fund, Prince of Songkla university (Grant No.: ENG6204107S) and the new strategic research project (P2P), Walailak University, Thailand.

ORCID

Kittipong Kunchariyakun  <http://orcid.org/0000-0002-7025-9419>

References

- [1] Taylor HFW. Cement chemistry. 2nd ed. London: Thomas Telford Services Ltd.; 1998.
- [2] Kurdowski W, Duszak S, Trybalska B. Belite produced by means of low-temperature synthesis. *Cem Concr Res.* 1997;27(1):51–62.
- [3] Bouzidi MA, Tahakourt A, Bouzidi N, et al. Synthesis and characterization of belite cement with high hydraulic reactivity and low environmental impact. *Arab J Sci Eng.* 2014;39(12):8659–8668.
- [4] Odler I. Special inorganic cements. New York: Simultaneously; 2000.
- [5] Roy DM, Oyefesobi SO. Preparation of very reactive Ca₂SiO₄ powder. *J Am Ceram Soc.* 1977;60(3–4): 178–180.
- [6] El-Didamony H, A. Khalil K, A.Ahmed I, et al. Preparation of β -dicalcium silicate (β -C₂S) and calcium sulfoaluminate (C₃A₃CS₂) phases using non-traditional nano-materials. *Constr Build Mater.* 2012;35:77–83.
- [7] Sinyoung S, Kunchariyakun K, Asavapisit S, et al. Synthesis of belite cement from nano-silica extracted from two rice husk ashes. *J Environ Manage.* 2017;190:53–60.

- [8] Rungchet A, Chindaprasirt P, Wansom S, et al. Hydrothermal synthesis of calcium sulfoaluminate–belite cement from industrial waste materials. *J Cleaner Prod.* 2016;115:273–283.
- [9] Pimraksa K, Hanjitsuwan S, Chindaprasirt P. Synthesis of belite cement from lignite fly ash. *Ceram Int.* 2009;35(6):2415–2425.
- [10] Singh NB. Hydrothermal synthesis of β -dicalcium silicate (β -Ca₂SiO₄). *Prog Cryst Growth Charact Mater.* 2006;52(1–2):77–83.
- [11] Antonović V, Pundienė I, Stonys R, et al. A review of the possible applications of nanotechnology in refractory concrete. *J Civ Eng Manag.* 2010;16(4):595–602.
- [12] Hosseini P, Mohamad MI, Nekooie MA, et al. Toward green revolution in concrete industry: the role of nanotechnology (a review). *Aust J Basic Appl Sci.* 2011;5(12):2768–2782.
- [13] Pacheco-Torgal F, Miraldo S, Ding Y, et al. Targeting HPC with the help of nanoparticles: an overview. *Constr Build Mater.* 2013;38:365–370.
- [14] Jo B-W, Kim C-H, Tae G-h, et al. Characteristics of cement mortar with nano-SiO₂ particles. *Constr Build Mater.* 2007;21(6):1351–1355.
- [15] Singh LP, Karade SR, Bhattacharyya SK, et al. Beneficial role of nanosilica in cement based materials – a review. *Constr Build Mater.* 2013;47:1069–1077.
- [16] Santra AK, Boul P, Pang X. Influence of nanomaterials in oilwell cement hydration and mechanical properties. SPE: Society of Petroleum Engineers; 2012: SPE 156937: 1-13.
- [17] Korpa A, Trettin R, Böger KG, et al. Pozzolanic reactivity of nanoscale pyrogene oxides and their strength contribution in cement-based systems. *Adv Cem Res.* 2008;20(1):35–46.
- [18] Rodríguez ED, Bernal SA, Provis JL, et al. Structure of Portland cement pastes blended with sonicated silica fume. *J Mater Civ Eng.* 2012;24(10):1295–1304.
- [19] Ivorra S, Garcés P, Catalá G, et al. Effect of silica fume particle size on mechanical properties of short carbon fiber reinforced concrete. *Mater Des.* 2010;31(3):1553–1558.
- [20] Maas AJ, Ideker JH, Juenger MCG. Alkali silica reactivity of agglomerated silica fume. *Cem Concr Res.* 2007;37(2):166–174.
- [21] Teixeira SR, Magalhães RS, Arenales A, et al. Valorization of sugarcane bagasse ash: producing glass-ceramic materials. *J Environ Manage.* 2014;134:15–19.
- [22] Faria KCP, Gurgel RF, Holanda JNF. Recycling of sugarcane bagasse ash waste in the production of clay bricks. *J Environ Manage.* 2012;101:7–12.
- [23] Madurwar MV, Mandavgane SA, Ralegaonkar RV. Development and feasibility analysis of bagasse ash bricks. *J Energy Eng.* 2015;141(3):04014022.
- [24] Kunchariyakun K, Asavapisit S, Sombatsompop K. Properties of autoclaved aerated concrete incorporating rice husk ash as partial replacement for fine aggregate. *Cem Concr Compos.* 2015;55:11–16.
- [25] Villar-Cociña E, Valencia-Morales E, González-Rodríguez R, et al. Kinetics of the pozzolanic reaction between lime and sugar cane straw ash by electrical conductivity measurement: a kinetic–diffusive model. *Cem Concr Res.* 2003;33(4):517–524.
- [26] Cordeiro GC, Toledo Filho RD, Fairbairn EMR. Effect of calcination temperature on the pozzolanic activity of sugar cane bagasse ash. *Constr Build Mater.* 2009;23(10):3301–3303.
- [27] Abbas S, Kazmi SMS, Munir MJ. Potential of rice husk ash for mitigating the alkali-silica reaction in mortar bars incorporating reactive aggregates. *Constr Build Mater.* 2017;132:61–70.
- [28] Van V-T-A, Rößler C, Bui D-D, et al. Pozzolanic reactivity of mesoporous amorphous rice husk ash in portlandite solution. *Constr Build Mater.* 2014;59:111–119.
- [29] Van V-T-A, Rößler C, Bui D-D, et al. Mesoporous structure and pozzolanic reactivity of rice husk ash in cementitious system. *Constr Build Mater.* 2013;43:208–216.
- [30] Bakaev VA, Pantano CG. Inverse reaction chromatography. 2. Hydrogen/deuterium exchange with silanol groups on the surface of fumed silica. *J Phys Chem C.* 2009;113(31):13894–13898. 2009/08/06
- [31] Ge J, Huynh T, Hu Y, et al. Hierarchical magnetite/silica nanoassemblies as magnetically recoverable catalyst-supports. *Nano Lett.* 2008;8(3):931–934.
- [32] Morpurgo M, Teoli D, Pignatto M, et al. The effect of Na₂CO₃, NaF and NH₄OH on the stability and release behavior of sol-gel derived silica xerogels embedded with bioactive compounds. *Acta Biomater.* 2010;6(6):2246–2253.
- [33] Carmona VB, Oliveira RM, Silva WTL, et al. Nanosilica from rice husk: extraction and characterization. *Ind Crops Prod.* 2013;43:291–296.
- [34] Vaibhav V, Vijayalakshmi U, Roopan SM. Agricultural waste as a source for the production of silica nanoparticles. *Spectrochim Acta A Mol Biomol Spectrosc.* 2015;139:515–520.
- [35] Amnadnua K, Tangchirapat W, Jaturapitakkul C. Strength, water permeability, and heat evolution of high strength concrete made from the mixture of calcium carbide residue and fly ash. *Mater Des.* 2013;51:894–901.
- [36] Jaturapitakkul C, Roongreung B. Cementing material from calcium carbide Residue-Rice husk ash. *J Mater Civ Eng.* 2003;15(5):470–475.
- [37] Krammart P, Tangtermsirikul S. Properties of cement made by partially replacing cement raw materials with municipal solid waste ashes and calcium carbide waste. *Constr Build Mater.* 2004;18(8):579–583.
- [38] Wang YL, Dong SJ, Liu LL, et al. Using calcium carbide slag as one of calcium-containing raw materials to produce cement clinker. *MSF.* 2013;743–744:171–174.
- [39] Makaratat N, Jaturapitakkul C, Namarak C, et al. Effects of binder and CaCl₂ contents on the strength of calcium carbide residue-fly ash concrete. *Cem Concr Compos.* 2011;33(3):436–443.
- [40] Somna K, Jaturapitakkul C, Kajitvichyanukul P. Microstructure of calcium carbide residue–ground fly ash paste. *J Mater Civ Eng.* 2011;23(3):298–304.
- [41] American Society for Testing Materials. ASTM C114: standard test methods for chemical analysis of hydraulic cement. Philadelphia, PA.
- [42] American Society for Testing Materials. ASTM C109/C109M-20b: standard test method for compressive strength of hydraulic cement mortars (using 2-in. or [50 mm] cube specimens). Philadelphia, PA.
- [43] Arif E, Clark MW, Lake N. Sugar cane bagasse ash from a high efficiency co-generation boiler: applications in cement and mortar production. *Constr Build Mater.* 2016;128:287–297.
- [44] Liou T-H, Yang C-C. Synthesis and surface characteristics of nanosilica produced from alkali-extracted rice husk ash. *Mater Sci Eng B.* 2011;176(7):521–529. 2
- [45] Kurdowski W. *Cement and concrete chemistry.* Netherlands: Springer; 2014.
- [46] Yannaquis N, Guinier A. Polymorphic B-Y transition of calcium orthosilicate. *Bull Soc Franc Miner Crist.* 1959;82:126.
- [47] Gawlicki M. Studies of calcium orthosilicate polymorphism by differential thermal analysis. *J Therm Anal.* 1987;32(6):1723–1725.
- [48] The American Ceramics Society. *Progress in nanotechnology applications.* New Jersey: Wiley; 2010.

- [49] Ewais EMM, Ahmed YMZ, El-Amir AAM, et al. Cement kiln dust–quartz derived wollastonite ceramics. *J Ceram Soc Japan*. 2015;123(1439):527–536.
- [50] Abd Rashid R, Shamsudin R, Abdul Hamid MA, et al. Low temperature production of wollastonite from limestone and silica sand through solid-state reaction. *J Asian Ceram Soc*. 2014;2(1):77–81.
- [51] Pontikes Y, Jones P, Geysen D, et al. Options to prevent dicalcium silicate-driven disintegration of stainless steel slags. *Arch Metall Mater*. 2010;55(4):1167–1172.
- [52] Thilo E, Funk H. Chemische untersuchungen von silicaten. *Z Anorg Allg Chem*. 1953;273(1–2): 28–40.
- [53] Kumar D, Maiti SC, Ghoroi C. Decomposition kinetics of CaCO₃ dry coated with nano-silica. *Thermochim Acta*. 2016;624(Supplement C):35–46.
- [54] Ávalos-Rendón TL, Chelala EAP, Mendoza Escobedo CJ, et al. Synthesis of belite cements at low temperature from silica fume and natural commercial zeolite. *Mater Sci Eng B*. 2018;229:79–85.